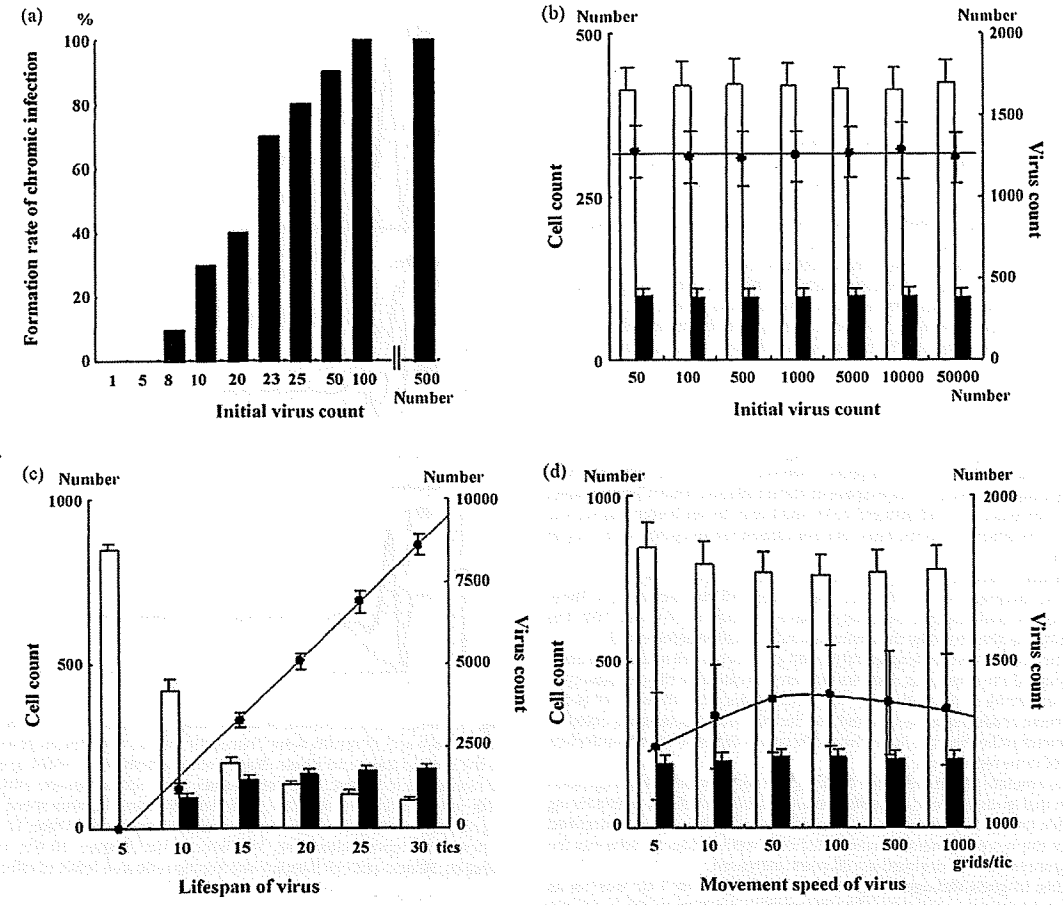

Fig. 4. Effects of changes in viral parameters. (a) The higher the initial virus count, the greater is the increase in the rate of formation of chronic infection, but (b) there was no effect on the conditions in the equilibrium phase. (c) Extending the virus lifespan increased the virus count. (d) Increasing the speed of virus movement to 100 grids/tic increased the virus count, but increasing it to 500 grids/tic had the opposite effect, with a slight declining trend. (a) Black bars: number of infections produced; (b–d) black circles: virus count; line: virus count approximation curve; white bars: uninfected cell count; black bars: infected cell count.

established. When the simulation was performed multiple times, the features described above were maintained, and the average values for virus, infected cell, and uninfected cell counts during the equilibrium state were all consistent.

Fig. 1d shows the simulation screen of the RePast. When we attempted setting all the initial parameters to the same values as those in the StarLogo, the results were not consistent. When we recalculated the parameters from the simulation results, in RePast, the parameters were largely maintained at the levels of the settings, but in StarLogo, the lifespans of both cell types became shorter than the settings while the simulation was in progress. We made the results of both simulations consistent by using the same parameters during the actual simulation (Fig. 2a and b).

3.2. Comparison Between Agent-based Simulation Models and Mathematical Simulation Model

We investigated whether the results of a chronic viral infection disease model produced by RePast would be consistent with the results of a mathematical model. For the mathematical model, we carried out an approximate integration using a four-dimensional Runge–Kutta method to ensure that the uninfected cell count and infected cell count would be in the same class. Parameters were always fixed as constant between simulations. The simulation results were consistent for the equilibrium phase, but transitions in virus count during the transient phase varied, with a shift to equilibrium state following two overshoots in the mathematical model, but a monotonic increase following a logistic curve in the agent-based model (Fig. 3). In the mathematical model, when the equilibrium condition was calculated with $dT/dt = dI/dt = dV/dt = 0$, the equilibrium-phase virus count, uninfected cell count, and infected cell count were very similar to those of the agent-based model (virus count: mathematical model 371.8/space, agent-based model 371.1 ± 32.4/space [average ± SD]; uninfected cell count: mathematical model 1605/space, agent-based model 1454 ± 194/space; infected cell count: mathematical model 115.9/space, agent-based model 108.3 ± 14.2/space).

3.3. Usability of the Models; Effect of Changing Parameters

We investigated the changes in the equilibrium phase brought about by changing each parameter. All the investigations below were carried out by using RePast, and we used the average values from ten simulations.

3.4. Viral Parameters

The lower the virus counts at the beginning of the simulation, the lower the probability of a chronic infection (Fig. 4a). However, the initial virus count did not have any effect on the equilibrium

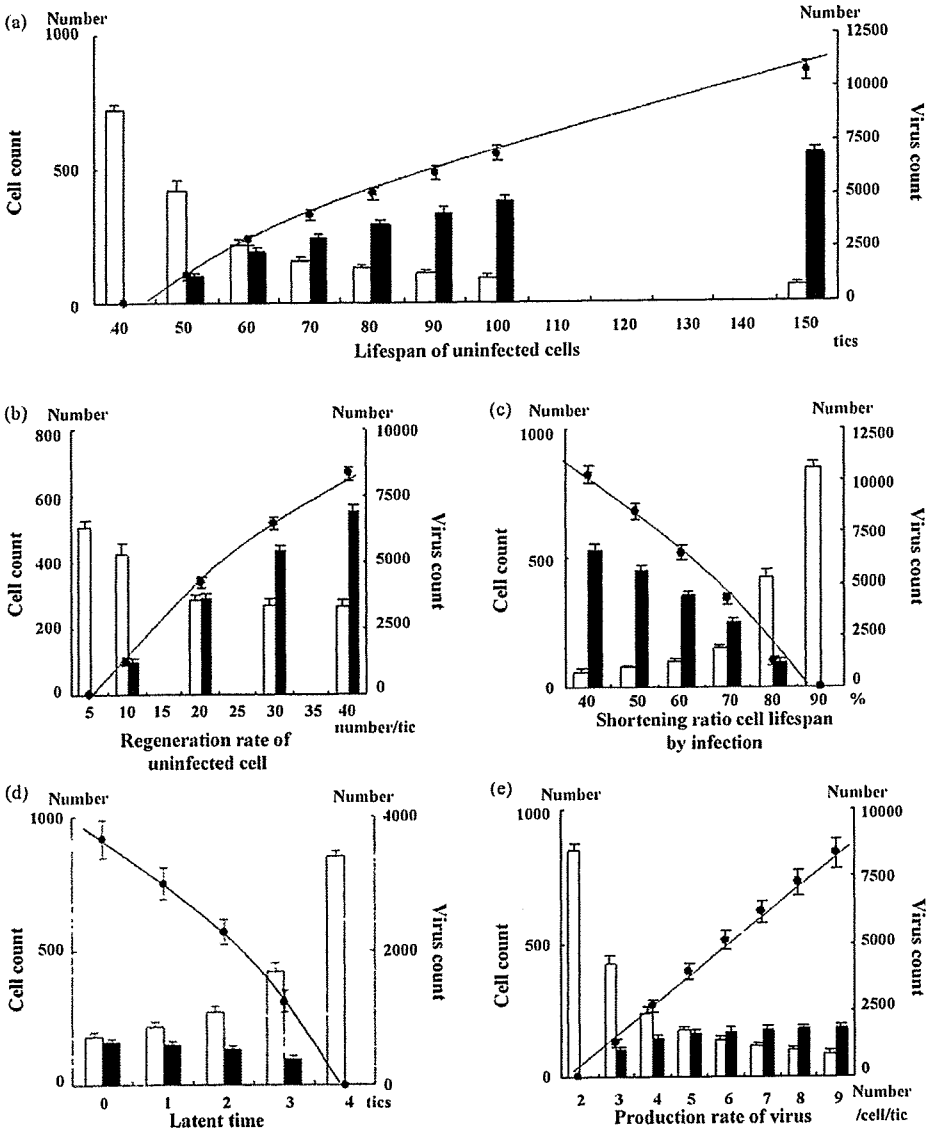

Fig. 5. Effects of changes in cell parameters. (a) Extending the uninfected cell lifespan and (b) increasing the uninfected cell regeneration rate increased the virus count. (c) Raising the lifespan-shortening ratio as a result of infection shortened the lifespan of infected cells, thereby decreasing the virus count. (d) Extending the latent period shortened the period of virus production from infected cells, thereby decreasing the virus count. (e) Increasing the virus production count resulted in a linear increase in equilibrium-phase virus count. Black circles: virus count; line: virus count approximation curve; white bars: uninfected cell count; black bars: infected cell count.

phase itself (Fig. 4b). Extending the lifespan of viruses resulted in a linear increase in equilibrium-phase virus count (Fig. 4c). Although the infected cell count increased, the rate of increase gradually declined. Changing the speed of viral movement resulted in the equilibrium-phase virus count to eventually decline after 100 grids/tic was reached, allowing movement over an area twice the size of the simulation space (Fig. 4d).

3.5. Uninfected Cell Parameters

Extending the lifespan of uninfected cells led to an increased virus count during the equilibrium phase (Fig. 5a). Increasing the uninfected cell regeneration rate also contributed to increased equilibrium-phase virus count (Fig. 5b). In both the cases, the increases in virus count and infected cell count were not linear, but showed a tendency for the rate of increase to decline gradually.

3.6. Infected Cell Parameters

We carried out an investigation of the effects of variation in the lifespan-shortening ratio on the virus count on the assumption that cell lifespan is shortened by infection. When this ratio was increased, the virus count decreased (Fig. 5c). An extended latent period was also related to a decreased virus count (Fig. 5d). However, the virus production from infected cells led to a linear increase in the virus count (Fig. 5e).

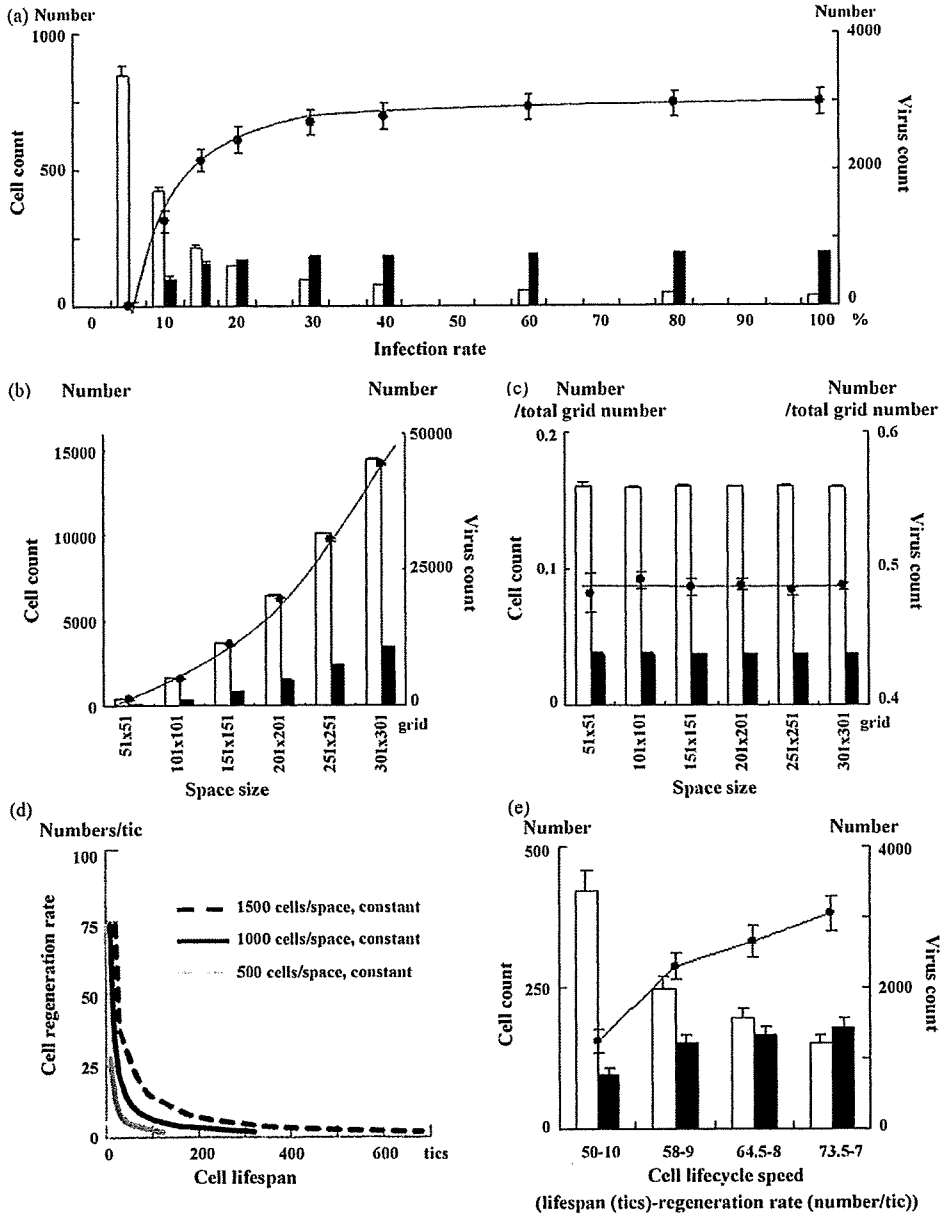

Fig. 6. (a) Increasing the infection rate increased the virus count in equilibrium periods, but the virus count did not change at infection rates of 30% or more. (b) The size of the simulation space increased not only virus count but also the cell count; however, (c) when virus and cell counts were divided by the total number of grids in the space, they were constant for all space sizes. (d) Changing the lifespan and regeneration rate of uninfected cells in opposite directions at the same time makes it possible to change only the cell cycle speed without altering the uninfected cell count. (e) When the cell cycle speed was reduced, the virus count increased toward the right of the graph. This may be because the effect of extending the lifespan of cells exceeds that of reducing their regeneration rate. (a–c and e) Black circles: virus count; line: virus count approximation curve; white bars: uninfected cell count; black bars: infected cell count.

3.7. Infection Rate and Space Size

Increasing the infection rate caused an increase in the virus count, but the change was minimal at an infection rate of 30% or more. The same results were seen for infected cell count, but a decrease in uninfected cell count resulted in a tendency for the infection rate to decrease by up to 60% (Fig. 6a).

The larger the space, higher the increase in both virus and cell counts (Fig. 6b). This increase was proportional to space size, however, when virus and cell counts were divided by the total number of grids in the space they were all constant (Fig. 6c).

3.8. Cell Cycle Speeds

Running a simulation with the initial virus count set to zero enables only the equilibrium condition for uninfected cells to be simulated. Changing the lifespan and regeneration rate of uninfected cells in opposite directions at the same time makes it possible

to change the cell cycle speed without altering the uninfected cell count (Fig. 6d). We used this technique to investigate how changing the cell cycle speed affected the equilibrium phase. Fig. 6e shows the results. Cell lifespan increases while the cell cycle speed declines. The equilibrium virus count increased in accordance with slower cell cycle speeds.

4. Discussion

In this study, we investigated the models using two agent-based simulation methods to program a simple virus–host chronic infection model. The same model written in two different programming language systems displayed the same results. The transient phase was unlike that seen in a mathematical simulation with no overshoot in virus count, but rather a smooth transition to the equilibrium phase. The virus count at the start of the simulation only had effect on the rate of infection development. Increases in virus lifespan, uninfected cell lifespan, uninfected cell regeneration rate, virus production count from infected cells, and infection rate all led to increased equilibrium-phase virus count. Rises in the infected cell lifespan-shortening ratio, latent period, and cell cycle speed decreased the equilibrium-phase virus count. The size of the space itself had no innate effect on the equilibrium phase, but a speed of movement of the virus that was twice the size of the space produced the maximum virus count.

Reproducibility is the basis for all scientific study, but there are many problems to prove it in computer simulations, such as programming bugs. As agent-based simulation deals with numerous agents individually, it requires vast amounts of calculations. Accumulation of very small change of values leads to large differences of results. In this study, we investigated two programs based on two programming languages to confirm the reproducibility of our simulation results in different programming languages. The results of two simulations were consistent, but in StarLogo, the lifespan parameters had a tendency to be lower than when they were set while simulations were actually in progress. This may be because the number of digits used in calculations was different between the two programs. RePast performs calculations to at least eight decimal places. In StarLogo, the library settings only enable settings to be made up to five decimal places. It is probable that these small differences accumulate during repeated calculations and are reflected in the simulation. Ultimately, we confirmed that the differences in results obtained by using different libraries and programming languages were not innate and by making the parameters consistent during simulation, consistent results were obtained.

Mathematical models using formulae for HIV therapy was published in 1994, the method has since been applied to HBV and HCV (Ho et al., 1995; Nowak et al., 1996; Neumann et al., 1998), and they were thought to be good reflections of the reality. In the mathematical model, viruses and cells are conceived as individuals in the concept itself, but both of them are perceived *en masse* when calculations are performed. However a feature of the agent-based simulation is that it deals with individual viruses and cells as separate agents. By moving each agent individually, it probes the factors influencing overall shifts from the micro viewpoint. When the space is viewed as a whole, it is possible to watch on the screen the collective movement of groups of agents. Recently, models that provide a visual representation of Epstein-Barr virus and HIV infection have been reported, both of which are useful for an instinctive and intuitive understanding (Duca et al., 2007; Shapiro et al., 2008; Castiglione et al., 2007).

In agent-based simulation model, virus count transit smoothly to the equilibrium phase. On the other hand, virus counts overshoot during transient phase in mathematical model. We think this difference is derived from technicality of different modeling. The difference in concepts between mathematical models and agent-based models is the space. The mathematical model has no space in concept, but agents move across the space in the agent-based model. In agent-based models, the densities of virus and cells change overtime especially in the transition phase because of the limited space. These changes of the densities of virus and cells lead to the dynamic change of the encounter rate of viruses and cells. The mathematical model does not make such concept of the density; the encounter rate is constant. This may be the reason for the difference between two models in the transition phase. Since no overshoot of virus counts in transient phase had been reported from in vivo studies of hepatitis C virus and simian immunodeficiency virus (Dahari et al., 2005; Nowak et al., 1997), agent-based model correlates with actual biology in vivo at least for these viruses. The increase of initial virus count at the start of simulation correlates with higher encounter rate of viruses and cells which make the linear increasing of infection forming rate. Mathematical model can only express the infection formation rate as "infected or not".

The importance of viral passing speed in the agent-based model is also explained by the "space". Although the virus actually moves through the blood stream in our body and virus could not decide their moving speeds by themselves, there is most appropriate speed for virus to meet the cells on the simulation space by the highest probability. The effect of cell cycle speed should be mentioned by another affection of the space. A fast cell cycle speed means that the lifespan of uninfected cells is short. Then fast cell cycle speed leads to the short lifespan of infected cells. A higher regeneration rate for uninfected cells results in a higher rate of infection among uninfected cells by viruses, but in situations where viruses and cells are dispersed around the space this is ineffective in increasing the infection rate, as the latter depends on the probability that they will encounter one another. As a result, the infected cell count decreases during the equilibrium phase, as does the virus count.

In this study, we confirmed the reproducibility and usability of agent-based models in expressing the interaction between viruses and cells. A feature of this simulation system is that it uses the concept of space as actual space, which means that the existence of the space becomes an additional controlling factor on the simulation results. This is a concept that is absent from mathematical models. The reality is that we have a spatial existence, and an advantage of the agent-based simulation system is the fact that it accounts for the space. Another feature of the simulation system is that it enables the condition to be perceived in visual terms, making it easy to understand. However it may be affected by computer performance and by the limitations of programming languages or the program itself, this system may offer a powerful tool for the future analysis of real virus–host interaction disease.

Conflict of interest

No conflicts of interest exist for all authors.

References

Castiglione, F., Pappalardo, F., Bernaschi, M., Motta, S., 2007. Optimization of HAART with genetic algorithms and agent-based models of HIV infection. Bioinformatics 23, 3350–3355, doi:10.1093/bioinformatics/btm408.

Dahari, H., Major, M., Zhang, X., Mihalik, K., Rice, C.M., Perelson, A.S., Feinstone, S.M., Neumann, A.U., 2005. Mathematical modeling of primary hepatitis c infection: noncytolytic clearance and early blockage of virion production. Gastroenterology 128, 1056–1066, doi:10.1053/j.gastro.2005.01.049.

Duca, K.A., Shapiro, M., Delgado-Eckert, E., Hadinoto, V., Jarrah, A.S., Laubenbacher, R., Lee, K., Luzuriaga, K., Polys, N.F., Thorley-Lawson, D.A., 2007. A virtual look at Epstein-Barr virus infection: biological interpretations. PLoS Pathog. 3, 1388–1400, doi:10.1371/journal.ppat.0030137.

Gilbert, N., Bankes, S., 2002. Platforms and methods for agent-based modelling. Proc. Natl. Acad. Sci. U.S.A. 99 (Suppl. 3), 7197–7198.

Ho, D.D., Neumann, A.U., Perelson, A.S., Chen, W., Leonard, J.M., Markowitz, M., 1995. Rapid turnover of plasma virions and CD4 lymphocytes in HIV-1 infection. Nature 373, 123–126, doi:10.1038/373123a0.

Naniche, D., 2009. Human immunology of measles virus infection. Curr. Top. Microbiol. Immunol. 330, 151–171.

Neumann, A.U., Lam, N.P., Dahari, H., Gretch, D.R., Wiley, T.E., Layden, T.J., Perelson, A.S., 1998. Hepatitis C viral dynamics in vivo and the antiviral efficacy of interferon-alpha therapy. Science 282, 103–107, doi:10.1126/science.282.5386.103.

Nowak, M.A., Bonhoeffer, S., Hill, A.M., Boehme, R., Thomas, H.C., McDade, H., 1996. Viral dynamics in hepatitis B virus infection. Proc. Natl. Acad. Sci. U.S.A. 93, 4398–4402.

Nowak, M.A., Lloyd, A.L., Vasquez, G.M., Wiltrout, T.A., Wahl, L.M., Biscofberger, N., Williams, J., Kinter, A., Fauci, A.S., Hirsch, V.M., Lifson, J.D., 1997. Viral dynamics of primary viremia and antiretroviral therapy in simian immunodeficiency virus infection. J. Virol. 71, 7518–7525.

Shapiro, M., Duca, K.A., Lee, K., Delgado-Eckert, E., Hawkins, J., Jarrah, A.S., Laubenbacher, R., Polys, N.F., Hadinoto, V., Thorley-Lawson, D.A., 2008. A virtual look at Epstein-Barr virus infection: simulation mechanism. J. Theor. Biol. 252, 633–648, doi:10.1016/j.jtbi.2008.01.032.

See, H., Wark, P., 2008. Innate immune response to viral infection of the lungs. Paediatr. Respir. Rev. 9, 243–250, doi:10.1016/j.prrv.2008.04.001.

J Gastroenterol (2009) 44:952–963
DOI 10.1007/s00535-009-0087-x

ORIGINAL ARTICLE—LIVER, PANCREAS, AND BILIARY TRACT

Predictive values of amino acid sequences of the core and NS5A regions in antiviral therapy for hepatitis C: a Japanese multi-center study

Takeshi Okanoue · Yoshito Itoh · Hiroaki Hashimoto · Kohichiroh Yasui · Masahito Minami · Tetsuo Takehara · Eiji Tanaka · Morikazu Onji · Joji Toyota · Kazuaki Chayama · Kentaro Yoshioka · Namiki Izumi · Norio Akuta · Hiromitsu Kumada

Received: 31 March 2009 / Accepted: 20 April 2009 / Published online: 11 June 2009

Abstract

Background Chronic hepatitis C (CHC) genotype 1b patients with high viral load are resistant to peginterferon (PEG-IFN) and ribavirin (RBV) combination therapy, especially older and female patients.

Methods To elucidate the factors affecting early and sustained viral responses (EVR and SVR), 409 genotype 1b patients CHC with high viral loads who had received 48 weeks of PEG-IFN/RBV therapy were enrolled. The amino acid (aa) sequences of the HCV core at positions 70 and 91 and of the interferon sensitivity determining region (ISDR) were analyzed. Host factors, viral factors, and treatment-related factors were subjected to multivariate analysis.

Results Male gender, low HCV RNA load, high platelet count, two or more aa mutations of ISDR, and wild type of core aa 70 were independent predictive factors for SVR. In patients with over 80% adherences to both PEG-IFN and RBV, male gender, mild fibrosis stage, and wild type of core aa 70 were independent predictors for SVR.

Conclusions Independent predictive factors for SVR were: no aa substitution at core aa 70, two or more aa mutations in the ISDR, low viral load, high values of platelet count, mild liver fibrosis and male gender.

T. Okanoue (✉)
Hepatology Center, Saiseikai Suita Hospital,
1-2 Kawazonocho, Suita 564-0013, Japan
e-mail: okanoue@suita.saiseikai.or.jp

T. Okanoue Y. Itoh H. Hashimoto K. Yasui M. Minami
Department of Gastroenterology and Hepatology,
Kyoto Prefectural University of Medicine,
Kawaramachi-Hirokoji Kamigyo-Ku,
Kyoto 602-8566, Japan

Y. Itoh
e-mail: yitoh@koto.kpu-m.ac.jp

H. Hashimoto
e-mail: road1820@yahoo.co.jp

K. Yasui
e-mail: yasuik@koto.kpu-m.ac.jp

M. Minami
e-mail: minami@koto.kpu-m.ac.jp

T. Takehara
Department of Gastroenterology and Hepatology,
Osaka University Graduate School of Medicine,
2-2 Yamadaoka, Suita 565-0871, Japan
e-mail: takehara@gh.med.osaka-u.ac.jp

E. Tanaka
Department of Medicine, Shinshu University School
of Medicine, 3-1-1 Asahi, Matsumoto 390-8621, Japan
e-mail: etanaka@shinshu-u.ac.jp

M. Onji
Department of Gastroenterology, Ehime University,
454 Shizukawa, Tohon, Ehime 791-0295, Japan
e-mail: onjimori@m.med.ehime-u.ac.jp

J. Toyota
Departmet of Gastroenterology, Sapporo-Kosei General
Hospital, Kita Sanjyo, Chuo-ku, Sapporo 060-0033, Japan
e-mail: joji.toyota@ja_hokkaidoukouseiren.or.jp

K. Chayama
Department of Medicine and Molecular Science,
Graduate School of Science, Hiroshima University,
1-2-3 Kasumi, Minami-ku, Hiroshima,
Hiroshima 734-8551, Japan
e-mail: chayama@hiroshima-u.ac.jp

K. Yoshioka
Department of Hepato-Biliary-Pancreas, Fujita Health Science,
Kutsukake-cho, Toyoake 470-1192, Japan
e-mail: kyoshiok@fujita-hu.ac.jp

Keywords Chronic hepatitis C · Peginterferon and ribavirin · Core amino acid · Interferon sensitivity determining region

Abbreviations

CHC	Chronic hepatitis C
PEG-IFN	Peginterferon
RBV	Ribavirin
RVR	Rapid viral response
cEVR	Complete early viral response
LVR	Late viral response
ETR	End of treatment response
NR	Non response
SVR	Sustained viral response
ISDR	Interferon sensitivity determining region
Aa	Amino acid
ALT	Alanine aminotransferase
PLT	Platelet
HCC	Hepatocellular carcinoma

Introduction

A combination of pegylated interferon (PEG-IFN) and ribavirin (RBV) therapy for 48 weeks achieves a sustained viral response (SVR) rate of 40–50% in chronic hepatitis C (CHC) patients with a high viral load of genotype 1 [1–4]. The dose-reduction rate and the frequency of discontinuation of this treatment are high in aged patients [5]. The SVR rate of the therapy is lower in females than males, especially in older patients in Japan [6].

Around 30% of HCV carriers have serum alanine aminotransferase (ALT) levels within the upper limit of normal ranges [7, 8] and HCV carriers with persistently normal serum ALT (PNALT) and serum platelet (PLT) counts of over $15 \times 10^4/mm^3$ show low grade hepatic fibrosis and good prognosis [9]. Before treating HCV carriers, it is very important to predict non-response to PEG-IFN plus RBV therapy because of its medical cost, adverse effects, and its impact on the long term quality of life.

N. Izumi
Department of Gastroenterology and Hepatology, Musashino Red Cross Hospital, Sakaminamimachi, Musashino 180-8610, Japan
e-mail: nizumi@musashino.jrc.or.jp

N. Akuta H. Kumada
Department of Hepatology, Toranomon Hospital, Kajigaya, Takatsu-ku, Kawasaki 213-8587, Japan

N. Akuta
e-mail: akuta-gi@umin.ac.jp

H. Kumada
e-mail: kumahiro@toranomon.gr.jp

There are many factors affecting response to IFN monotherapy and PEG-IFN/RBV therapy, including body mass index (BMI) [10, 11], steatosis [12, 13], insulin resistance [14], stage of liver fibrosis [15, 16], total cholesterol (T. Chol), triglyceride (TG), adherence to both PEG-IFN and RBV [17], race [18, 19], age [1, 2, 20], and viral factors including serum quantity of HCV RNA, HCV genotype and substitution of amino acids (aa) in the interferon sensitivity determining region (ISDR, 2209–2248) of the nonstructural protein 5A (NS5A) [21] and in the core protein [22, 23]. Early viral response is an important predictive factor in PEG-IFN/RBV therapy for CHC patients with genotype 1 and high viral loads [24–27].

The aim of this study was to elucidate the valuable predictive factors of SVR in Japanese patients with HCV genotype 1b high viral loads following 48 weeks of PEG-IFN/RBV therapy, focusing on the relationship between aa substitutions in the ISDR and at core aa 70 and 91 and early viral kinetics.

Patients and methods

Selection of patients

This retrospective study was conducted at 15 clinical sites in Japan which are part of the Study Group of Optimal Treatment of Viral Hepatitis supported by the Ministry of Health, Labor and Welfare, Japan. Eligible subjects were CHC patients, who (1) had received liver biopsy; (2) were genotype 1b with high viral load ($\geq$100 KIU/ml by Cobas Amplicor Hepatitis C Virus Test, version 2.0) at the start of PEG-IFN/RBV therapy; (3) received weekly injections of PEG-IFN-α-2b (PEG-INTRON; Shering-Plough, Kenilworth, NJ) of 1.5 μg/kg bw and oral administration of RBV (Rebetol; Shering-Plough) for 48 weeks. The amount of RBV was adjusted based on the subject's body weight; (600 mg for $\leq$60 kg bw, 800 mg for 60–80 kg bw, 1,000 mg for > 80 kg bw); (4) were examined serially for quantitative and qualitative HCV RNA; and (5) the aa sequences at positions 70 and 91 in the core region and of the ISDR in the NS5A had been determined in pretreatment sera.

Hepatitis B virus (HBV) infection, human immunodeficiency virus (HIV) infection, autoimmune hepatitis, primary biliary cirrhosis, hemochromatosis, and Wilson's disease were excluded. Histopathological diagnosis was based on the scoring system of Desmet et al. [28]. The definition of alcohol abuse included patients having a history of more than 100 kg of total ethanol intake. Complete blood counts, liver function tests, serum lipids, serum ferritin, serum fibrosis markers, fasting plasma glucose (FPG), and immune reactive insulin (IRI) were examined in most cases. Written informed consent was obtained from all

patients before treatment, and the protocol was approved by the ethics committees in each site.

Study design

Four hundred and nine patients who completed 48 weeks of treatment and were followed for more than 24 weeks after treatment were enrolled in the first study (*Study design 1*).

To elucidate the effect of aa substitution of HCV core and in the ISDR on HCV dynamics, including a rapid viral response (RVR), complete early viral response (cEVR), a late viral response (LVR) and SVR, according to gender and age (<60 years $\geq$ 60 years), 201 of the 409 patients maintaining over 80% adherences to both PEG-IFN and RBV were enrolled in the second study (*Study design 2*).

Nucleotide sequencing of the core and NA5A gene

The nucleotide sequences encoding aa 1–191 (HCV core) and aa 2209–2248 (ISDR) were analyzed by direct sequencing as described by Akuta et al. [22, 27] and Enomoto et al. [21]. In brief, RNA was extracted from the sera and converted to cDNA and two nested rounds of polymerase chain reaction (PCR) were performed. Primers used in the PCR were as follows; (a) Nucleotide sequences of the core region: the first-round PCR was performed with CC11 (sense) and e14 (antisense) primers [22, 27], and the second-round PCR with CC9 (sense) and e14 (antisense) primers [22, 27]. (b) Nucleotide sequences of the ISDR in NS5A: the first-round PCR was performed with ISDR1 (sense) and ISDR2 (antisense) primers [21], and the second-round PCR with ISDR3 (sense) and ISDR4 (antisense) primers [21]. These sequences were compared with the consensus sequence of genotype 1b (HCV-J) [29]. Wild types virus encoded arginine and leucine at aa 70 and 91, respectively, and the aa substitutions were glutamine or histidine at aa 70 and methionine at aa 91.

Viral kinetic study

Serum HCV RNA levels were measured by PCR (Amplicor HCV RNA kit, version 2.0, Roche Diagnostics) using samples taken before treatment and at 4, 12, 24, and 48 weeks after the therapy. SVR was defined as HCV RNA negativity by qualitative analysis by PCR at 24 weeks after the treatment. RVR was defined as HCV RNA negativity at 4 weeks, cEVR as HCV RNA negativity at 12 weeks, LVR as HCV RNA negativity during 13–24 weeks and an end of treatment response (ETR) as HCV RNA negativity at the end of treatment. Patients who remained positive for HCV RNA at the end of the treatment and at 24 weeks after the therapy were defined as non-responders (NR).

Adherences to PEG-IFN and RBV

Adherences to PEG-IFN and RBV were assessed by separately calculating the actual doses of PEG-IFN and RBV received as percentages of the intended dosages. Adherences to PEG-IFN and RBV were divided into two groups; 80%$\leq$ and <80%.

Statistical analysis

All data analyses were conducted using the SAS version 9.1.3 statistical analysis packages (SAS Institute, Cary, NC, USA). Individual characteristics between groups were evaluated by Mann–Whitney U test for numerical variables or Fisher's exact test for categorical variables. Variables exhibiting values of $p < 0.1$ in the univariate analysis were subjected to stepwise multivariate logistic regression analysis. The grade of steatosis and iron deposition in liver tissue, BMI, albumin (Alb), low density lipoprotein-cholesterol (LDL-C), homeostasis model assesment-insulin resistance (HOMA-IR), ferritin, and hyaluronic acid were excluded from multivariate logistic regression analysis because of the absence of those data in more than 10% of the patients. All p values of $p < 0.05$ by the two-tailed test were considered statistically significant.

Results

Study design 1

Baseline backgrounds, characteristics and adherences of peginterferon and ribavirin in males and females

The treatment outcome of PEG-IFN and RBV combination therapy depends on gender in Japanese patients, so in addition to aa substitutions in the ISDR in NS5A [21] or at HCV core 70 and 91 [22, 27], we compared the baseline characteristics according to gender (Table 1). Males were younger and the grade of hepatic inflammation was milder in males. The serum levels of LDL-C, PLT count, and aa substitutions of ISDR and at core 70 and 91 did not differ significantly different between males and females. The frequency of no alcohol abuse was significantly ($p < 0.0001$) higher in females than males (Some of them are not described in Table 1).

The rates of over 80% adherences to PEG-IFN and RBV were significantly lower ($p = 0.0066$, $p < 0.00001$, respectively) in females than males. Only in those above 60 years did the rate of over 80% adherence to PEG-IFN not differ significantly between males and females, but the rate of over 80% adherence to RBV was significantly lower ($p = 0.035$) in females than males (Table 1).

Table 1 Backgrounds and characteristics of male and female patients

Factors	Gender		*p* value
	Male	Female	
No. of patients	256 (62.6%)	153 (37.4%)	
Age			
Median (range)	53 (18–73)	59 (23–75)	0.00001
F stage			
F0–2	206 (80.5%)	119 (77.8%)	0.592
F3–4	50 (19.5%)	34 (22.2%)	
Grade (A factor)			
A0–1	163 (63. 7%)	79 (51.6%)	0.026
A2–3	93 (36.3%)	74 (48.4%)	
HCV RNA load 0 week (KIU/mL)			
Median (range)	1500 (100–5000 <)	1280 (100–5000<)	0.384
ALT 0 week (IU/L)			
Median (range)	74.5 (16–504)	59 (19–391)	0.001
BMI			
Median (range)	23.6 (17.5–31.2)	22.1 (16.1–33.9)	0.00033
Alb (g/dL)			
Median (range)	4.0 (3.0–5.2)	3.8 (3.0–4.8)	0.011
LDL-C (mg/dL)			
Median (range)	97 (30–185)	90 (34–174)	0.612
T-Chol (mg/dL)			
Median (range)	167 (85–273)	176 (114–261)	0.0016
PLT count ($\times 10^4/mm^3$)			
Median (range)	17.0 (8.0–31.9)	16.4 (8.1–39.9)	0.350
Amino acid mutation of ISDR			
0–1	200 (78.1%)	121 (79.1%)	0.608
2≤	56 (21.9%)	32 (20.9%)	
Amino acid substitution of core 70			
Wild	177 (69.1%)	114 (74.5%)	0.261
Mutant	79 (30.9%)	39 (25.5%)	
Amino acid substitution of core 91			
Wild	153 (59.8%)	98 (64.1%)	0.403
Mutant	103 (40.2%)	55 (35.9%)	
PEG-IFN adherence			
<80%	41 (17.7%)	42 (30.4%)	0.0066
80%≤	190 (82.3%)	96 (69.6%)	
Ribavirin adherence			
<80%	54 (23.6%)	73 (52.1%)	<0.00001
80%≤	175 (76.4%)	67 (47.9%)	
Age: <60 years			
PEG adherence			
<80%	30 (17.8%)	23 (31.5%)	0.027
80%≤	139 (82.2%)	50 (68.5%)	
Ribavirin adherence			
<80%	27 (16.2%)	31 (42.5%)	0.000029
80%≤	140 (83.8%)	42 (57.5%)	
Age: 60 years≤			
PEG adherence			
<80%	11 (17.7%)	19 (29.2%)	0.147
80%≤	51 (82.3%)	46 (70.8%)	
Ribavirin adherence			
<80%	27 (43.5%)	42 (62.7%)	0.035
80%≤	35 (56.5%)	25 (37.3%)	

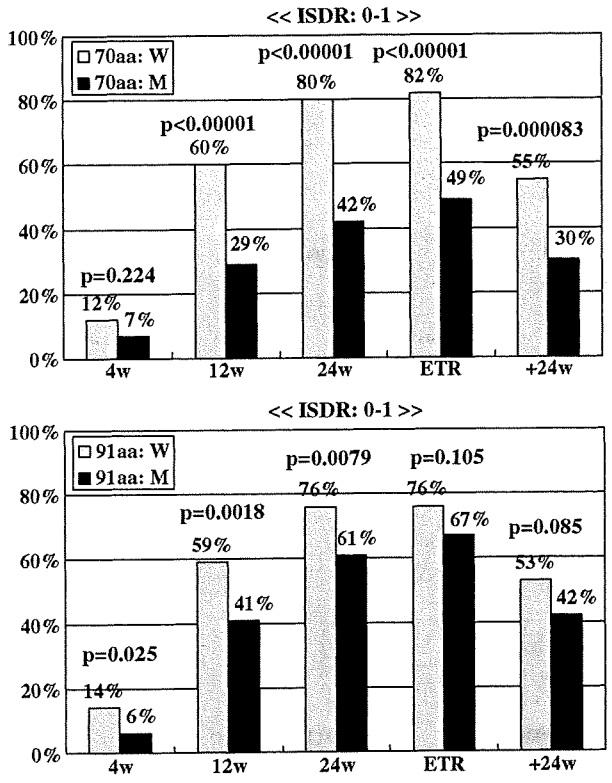

Fig. 1 Relationship between time course of serum HCV RNA negativity and amino acid substitutions in the ISDR and core amino acids 70 and 91. For cases with no or only one amino acid (aa) change in the ISDR, the rates of cEVR, LVR, ETR and SVR were significantly higher in patients with wild type core aa 70 but only the rates of RVR, cEVR, and LVR were significantly higher in patients with wild type core aa 91

Amino acid substitutions

There were no significant differences in the frequency of aa substitutions in the ISDR between males and females. Core aa substitutions at positions 70 and 91 were as follows; 291 (71.1%) were wild type and 118 (28.9%) were mutant at core aa 70, and 251 (61.4%) were wild type and 158 (38.6%) were mutant at core aa 91. There were no significant differences between males and females and between patients below and above 60 years of age.

Virological responses and aa substitutions

The rate of RVR did not differ significantly between males and females. However, more male patients showed HCV RNA negativity at 12 weeks (males vs. females; 60.7 vs. 48.4%, $p = 0.018$), 24 weeks (76.8 vs. 64.2%, $p = 0.0078$) and 48 weeks (78.2 vs. 68.6%, $p = 0.049$), and the proportion of male patients in SVR was significantly higher than that of females (61.3 vs. 37.3%, $p < 0.00001$).

RVR, cEVR and SVR rates were significantly higher in patients with two or more aa mutations in the ISDR compared to patients having no or one aa substitution in that region (20 vs. 11%, $p = 0.044$; 71 vs. 52%, $p = 0.0021$; 66 vs. 49%, $p = 0.0054$, respectively). AA substitution at core position 70 resulted in significantly lower rate of cEVR, LVR, ETR, and SVR (40 vs. 63%, $p = 0.000037$; 51 vs. 81%, $p < 0.00001$; 56 vs. 83%, 41 vs. 57%; $p < 0.00001$, $p = 0.0031$, respectively). Although the patients with the wild type aa at core 91 showed significantly higher rates of RVR and cEVR, the rate of SVR was not significantly higher in those patients ($p = 0.054$).

SVR rates were 30% for patients with no or one aa substitution in the ISDR and the core aa 70 substitution, and were significantly lower compared to those with the wild type aa core 70 (Fig. 1). These findings were not confirmed in patients with no or one aa substitution in the ISDR and the core aa 91 substitution (Fig. 1).

Factors affecting SVR by univariate analysis

Univariate analysis identified nine parameters that influenced non-SVR significantly: female gender, older age, advanced staged liver fibrosis, high viral load, low serum Alb level, low PLT count, no or one aa substitution in the ISDR, aa substitution at core aa 70, and low adherence to RBV (Table 2). The frequency of steatosis and HOMA-IR were significantly ($p = 0.0057$, $p < 0.00001$, respectively) lower in patients with SVR compared with non-SVR (data not shown). However, these factors were not entered in the multivariate analysis because of the absence of the data in many cases.

Factors affecting RVR, cEVR, and SVR by multivariate logistic regression analysis

Multivariate analysis identified four parameters that influenced RVR independently: low HCV RNA load, low serum ALT level, two or more aa mutations in the ISDR and the wild type aa at core position 91 (Table 3).

Concerning cEVR, male gender, mild fibrosis stage, low HCV RNA load, two or more aa mutations in the ISDR, and the wild type aa at core positions 70 and 91 were independent predictors (Table 3).

Concerning SVR, male gender ($p < 0.0001$), low HCV RNA load ($p = 0.013$), high PLT count ($p = 0.0019$), two or more aa mutations in the ISDR ($p = 0.024$), and wild type core aa 70 ($p = 0.0045$) were found to be independent predictors (Table 3).

The predictive values of the combination of gender, PLT count, ISDR and core aa 70 are shown in Fig. 2a. In male patients having PLT of $<15 \times 10^4/mm^3$, and, no or one aa substitution in the ISDR, the SVR rate was 68% when core 70

Table 2 Univariate analysis to identify the factors of SVR

Factors	Negative of HCV RNA after 24 weeks		*p* value
	(−)	(+)	
No. of patients	214 (52.3%)	195	
Gender			
Male	157 (61.3%)	99	<0.00001
Female	57 (37.3%)	96	
Age			
Median (range)	52.5 (18–75)	58 (20–74)	<0.00001
<60 years	155 (58.1%)	112	0.0018
60 years≤	59 (41.5%)	83	
Age: <60 years			
Male	118 (63.4%)	68	0.010
Female	37 (45.7%)	44	
Age: 60 years≤			
Male	39 (55.7%)	31	0.0011
Female	20 (27.8%)	52	
F stage			
F0–2	190 (58.5%)	135	0.000013
F3–4	25 (29.8%)	59	
Grade (A factor)			
A0–1	138 (56.8%)	104	0.130
A2–3	81 (48.5%)	86	
HCV RNA load 0 week (KIU/mL)			
Median (range)	1300 (100–5000<)	1700 (130–5000<)	0.016
ALT 0 week (IU/L)			
Median (range)	66 (16–391)	67 (19–504)	0.892
BMI			
Median (range)	23.0 (17.3–32.4)	23.25 (16.1–33.9)	0.714
Alb (g/dL)			
Median (range)	4.0 (3.2–5.2)	3.8 (3.0–4.8)	0.0088
LDL-C (mg/dL)			
Median (range)	94.5 (31–185)	97.5 (30–182)	0.611
T-Chol (mg/dL)			
Median (range)	169.5 (85–257)	170 (103–273)	0.511
PLT count ($\times 10^4/mm^3$)			
Median (range)	18.2 (8.7–39.9)	15.1 (8.0–31.9)	<0.00001
<15	54 (36.5%)	94	<0.00001
15≤	160 (61.3%)	101	
Amino acid mutation of ISDR			
0–1	156 (48.6%)	165	0.0054
2≤	58 (65.9%)	30	
Amino acid substitution of core 70			
Wild	166 (57.0%)	125	0.0031
Mutant	48 (40.7%)	70	
Amino acid substitution of core 91			
Wild	141 (56.2%)	110	0.054
Mutant	73 (46.2%)	85	
PEG-IFN adherence			
<80%	35 (42.2%)	48	0.063
80%≤	154 (53.8%)	132	
Ribavirin adherence			
<80%	55 (43.3%)	72	0.048
80%≤	132 (54.5%)	110	

Table 3 Multivariate logistic regression analysis to identify independent predictive factors of RVR, cEVR, and SVR

	Odds ratio	95% CI	*p* value
RVR factors selected by stepwise method			
F stage			
F0–2/F3–4	2.924	0.988–8.696	0.053
HCV RNA load 0 week (KIU/mL)			
<1000/1000≤	2.151	1.130–4.082	0.020
ALT 0 week (IU/L)			
<60/60≤	2.165	1.127–4.149	0.020
Amino acid mutation of ISDR			
2≤/0–1	2.371	1.187–4.735	0.014
Amino acid substitution of core 91			
W/M	2.137	1.021–4.464	0.044
cEVR factors selected by stepwise method			
Gender			
Male/female	1.912	1.209–3.021	0.0055
F stage			
F0–2/F3–4	2.079	1.133–3.817	0.018
HCV RNA load 0 week (KIU/mL)			
<1000/1000≤	1.608	1.002–2.577	0.049
PLT count ($\times 10^4/mm^3$)			
15≤/<15	1.427	0.882–2.309	0.148
Amino acid mutation of ISDR			
2≤/0–1	2.512	1.407–4.485	0.0018
Amino acid substitution of core 70			
W/M	2.513	1.508–4.184	0.0004
Amino acid substitution of core 91			
W/M	1.965	1.241–3.115	0.004
SVR factors selected by stepwise method			
Gender			
Male/female	3.704	2.132–6.410	<0.0001
F stage			
F0–2/F3–4	1.812	0.888–3.690	0.103
HCV RNA load0 week (KIU/mL)			
<1000/1000≤	2.024	1.163–3.534	0.013
PLT count ($\times 10^4/mm^3$)			
15≤/<15	2.469	1.394–4.372	0.0019
Amino acid mutation of ISDR			
2≤/0–1	2.148	1.107–4.170	0.024
Amino acid substitution of core 70			
W/M	2.415	1.316–4.444	0.0045
Amino acid substitution of core 91			
W/M	1.433	0.828–2.481	0.199
PEG adherence (%)			
80≤/<80	1.562	0.834–2.926	0.164

W Wild, *M* Mutant

was a wild type but only 16% in patients with mutant at core 70. In female patients, no or one aa substitution in ISDR and $<15 \times 10^4/mm^3$ of PLT count, the SVR rates were as low as 10 or 8%, irrespective of aa substitution at core 70. SVR was only 24% in patients with substitution of core aa 70 even when the PLT count was $\geq 15 \times 10^4/mm^3$. In this study, the combination analysis of PLT count, ISDR, and core aa substitution was useful for predicting non-SVR.

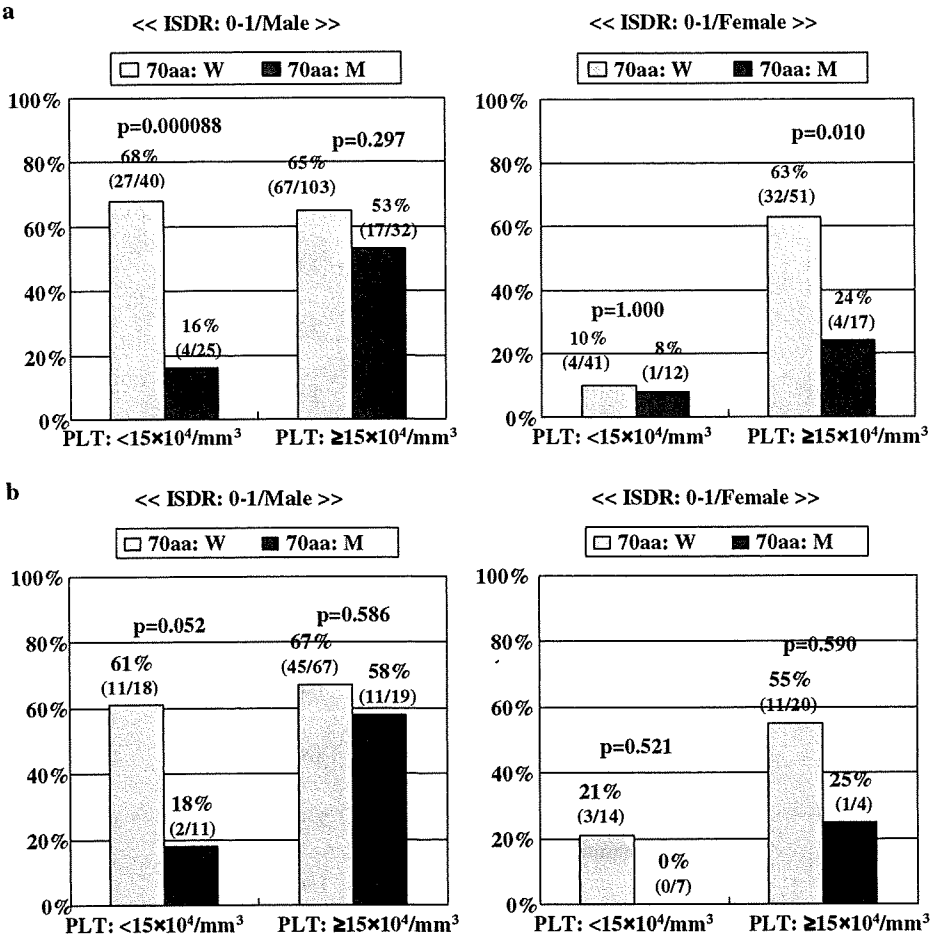

Fig. 2 Relationship between SVR rate and amino acid substitutions in the ISDR and core amino acids 70 and 91, PLT counts and gender difference. The two figures of **a** show the results of *Study 1* and the two figures of **b** show the results of *Study 2*. In male patients with no or only one amino acid (aa) substitution in the ISDR and PLT count of less than $15 \times 10^4/mm^3$, the SVR rate was 68% in those with wild type core aa 70, but only 16% in patients with mutant type of core aa 70, which is significantly different ($p = 0.000088$). There were no significant differences between wild type and mutant type of core aa 70 in the patients with no or one aa substitution in the ISDR and PLT count of over $15 \times 10^4/mm^3$. By contrast, in female patients with no or one aa substitution in the ISDR, there were no significant differences between wild type and mutant type of core aa 70 with PLT count of less than $15 \times 10^4/mm^3$, but there were significant differences between wild type and mutant type of core aa 70 with PLT counts of less than $15 \times 10^4/mm^3$ (**a**). For the patients maintaining over 80% adherences to both PEG-IFN and RBV, in males having no or one aa substitution in the ISDR and PLT counts of less than $15 \times 10^4/mm^3$, a wild type of core aa 70 could predict SVR with a positive predictive value (PPV) of 61% and negative predictive value (NPV) of 82% ($p = 0.052$). However, in male patients with PLT counts of over $15 \times 10^4/mm^3$, core aa 70 was not a useful marker for predicting SVR and non-SVR. The number of female patients with no or one aa substitution in ISDR was too small to reach a definite conclusion (**b**)

Study design 2

The basic features of 201 patients achieving 80% adherences to both PEG-IFN and RBV are as follows: the females were significantly ($p = 0.00006$) older than the males. Iron deposition in liver tissue, alcohol abuse, BMI, serum albumin level, serum ferritin level, and PLT count were significantly higher in males than females. Inflammatory activity was significantly ($p = 0.046$) higher in females than males (data not shown).

AA substitutions in the ISDR were as follows; in males 33 (22.3%) had two or more aa substitutions, in females 8 (15.1%) had two or more aa substitutions. The analysis of core aa position 70 and 91 sequences showed no significant differences in aa substitutions of either core aa 70 or 91 between males and females (data not shown).

In patients less than 60 years of age, SVR rate was significantly higher ($p = 0.0042$) in males than females, but no significant difference was noted between males and females over 60 years old. However, the number of patients over 60 years was small (Table 4).

Table 4 Univariate analysis to identify the significantly different factors between SVR and non-SVR (201 patients received over 80% adherences of both PEG-IFN and RBV)

Factors	Negative of HCV RNA after 24 weeks		*p* value
	(−)	(+)	
No. of patients	111 (55.2%)	90	
Gender			
Male	93 (62.8%)	55	0.00037
Female	18 (34.0%)	35	
Age			
Median (range)	51 (18–70)	56 (23–74)	0.00025
<60 years	91 (60.3%)	60	0.014
60 years≤	20 (40.0%)	30	
Age: <60 years			
Male	79 (66.4%)	40	0.0042
Female	12 (37.5%)	20	
Age: 60 years≤			
Male	14 (48.3%)	15	0.243
Female	6 (28.6%)	15	
F stage			
F0–2	103 (60.9%)	67	0.0012
F3–4	8 (25.8%)	23	
Grade (A factor)			
A0–1	80 (59.3%)	55	0.189
A2–3	31 (47.0%)	35	
HCV RNA load 0 week (KIU/mL)			
Median (range)	1300 (110–5000<)	1280 (130–5000<)	0.351
ALT 0 week (IU/L)			
Median (range)	74 (16–268)	67.5 (19–504)	0.752
BMI			
Median (range)	23.1 (17.3–31.0)	23.6 (16.1–33.9)	0.626
Alb (g/dL)			
Median (range)	3.95 (3.3–5.2)	3.9 (3.0–4.8)	0.079
LDL-C (mg/dL)			
Median (range)	96 (31–185)	97.5 (30–182)	0.865
T-Chol (mg/dL)			
Median (range)	170 (85–248)	170 (105–273)	0.624
PLT count ($\times 10^4/mm^3$)			
Median (range)	18.9 (8.7–30.9)	15.55 (7.2–28.4)	0.00003
<15	23 (35.9%)	41	0.00024
15≤	88 (64.2%)	49	
Amino acid mutation of ISDR			
0–1	84 (52.5%)	76	0.159
2≤	27 (65.9%)	14	
Amino acid substitution of core 70			
Wild	91 (61.5%)	57	0.0037
Mutant	20 (37.7%)	33	
Amino acid substitution of core 91			
Wild	73 (60.3%)	48	0.083
Mutant	38 (47.5%)	42	

Virological responses and aa substitution

The rates of RVR, cEVR, LVR, ETR and SVR in males and females were 12.5 versus 11.3% ($p = 1.000$), 59.6 versus 43.4% ($p = 0.053$), 74.3 versus 50.0% ($p = 0.0018$), 76.2 versus 66.7% ($p = 0.198$), and 62.8 versus 34.0% ($p = 0.00037$), respectively (data not shown). The backgrounds and characteristics of SVR and non SVR patients are shown in Table 4. There were significant differences in gender (male vs. female; $p = 0.00037$), age (<60 years vs. ≥60 years; $p = 0.014$), F stage (F0-2 vs. F3,4; $p = 0.0012$), PLT count ($<15 \times 10^4/mm^3$ vs. $15 \times 10^4/mm^3 \leq$; $p = 0.00024$), and substitution of core aa 70 (wild type vs. mutant, p = 0.0037) between SVR and non-SVR patients. The distribution of fatty change in liver tissue (≤10% vs. 11–33% vs. 34%≤; $p = 0.046$) and the grade of HOMA-IR (1.7 vs. 3.9, $p = 0.0018$) were significantly different between SVR and non-SVR (data not described in Table 4).

Factors affecting SVR by multivariate logistic regression analysis

Male gender ($p = 0.0006$), mild fibrosis stage ($p = 0.027$), and wild type of core aa 70 ($p = 0.043$) were independent predictors of SVR.

Valuable markers for predictions of sustained virological response to peginterferon and ribavirin therapy

Two or more aa mutations in the ISDR, wild type core aa 70, $\geq 15 \times 10^4/mm^3$ of PLT count, and male gender were selected statistically as independent predictors of SVR. We show here SVR rates of the patients having over 80% adherences to both PEG-IFN and RBV (Fig. 2b). In males having no or one aa substitution in the ISRD and PLT count of $<15 \times 10^4/mm^3$, wild type core aa 70 could predict SVR with a positive predictive value (PPV) of 61% and negative predictive value (NPV) of 82% ($p = 0.052$). In females, the SVR rate was very low in those who had substitution of core aa 70, but there was no significant difference between patients with wild type and substitution of core aa 70. The number of female patients was too small to provide a definite conclusion.

Discussion

The present multivariate logistic regression analysis revealed that male gender, low HCV RNA load, high PLT count, and two or more aa mutations in the ISDR and wild type core aa 70 were independent predictors for SVR. PLT count significantly decreased corresponding to the progression to the stage of liver fibrosis in CHC [9, 30, 31].

It has been considered that the low adherence level to PEG-IFN/RBV is a major cause of a significantly lower SVR rate in females and older patients [32]. The percentage of patients having over 80% adherences to both PEG-IFN and RBV was significantly lower in females than males, however, differences in the adherence to PEG-IFN/RBV between males and females were not independent predictive factors of non-SVR.

A recent report from Japan showed six or more mutations in the variable region 3 (V3) of nonstructural protein 5A (NS5A) plus upstream flanking region NS5A (aa 2334–2379), referred to as the IFN/RBV resistance determining region (IRRDR), was a useful marker for predicting SVR, but the ISDR sequence was not valuable for predicting SVR [33]. However, the number of subjects in that study was too small ($n = 45$) to reach an acceptable conclusion.

To elucidate the factors affecting low SVR rate in older female patients, we performed a multivariate logistic regression analysis using patients who achieved ≥80% adherence to both PEG-IFN and RBV. Male gender, stage of mild liver fibrosis, and wild type core aa 70 were independent predictors of SVR. In this study, blood concentration of RBV was determined in fewer than 50% of cases during treatment. Thus we cannot exclude the possibility of the effect of the blood concentration of RBV during treatment on the low SVR rate in females and older patients.

From the present analysis, it was clear that ALT, BMI, Alb, T. Chol, and adherence to RBV differed significantly between males and females, however, these factors were not independent predictors of SVR. There is a report that steatosis is an important cofactor that reduces the SVR rate in genotype 1 infected patients [34], however, such an effect was not seen in this study. Thus we could not identify the factors associated with a significantly lower SVR rate in females than males.

In the present multivariate logistic regression analyses, patients having wild type core aa 91 had significantly higher rates of RVR and cEVR, but not SVR, and patients with wild type core aa 70 had significantly higher rates of cEVR and SVR, but not RVR. Patients having two or more aa substitutions in the ISDR had significantly higher rates of RVR, cEVR, and SVR. Although several possibilities have been considered concerning the effects of aa substitutions of core protein on SVR in PEG-IFN/RBV therapy for CHC patients, the exact mechanisms have not yet been elucidated.

Recent reports have indicated that low serum IP-10 (interferon-γ inducible protein 10 kDa) [35], a higher HCV-specific CD8 cell proliferation potential [36], and a high ratio of Th1/Th2 [37] are good predictors of SVR to

PEG-IFN/RBV therapy. These results indicate the importance of immunological status and immunological response to treatment in patients difficult to treat with PEG-IFN/RBV therapy for CHC.

The present univariate analyses revealed that there were many factors relating to RVR, cEVR, and SVR including LDL-C, HOMA-IR, fatty change in liver tissue, and hyaluronic acid, however some of these factors had not been examined in some participating institutes. We consider that we must perform a prospective mass study using many factors including immunological aspects, viral factors, disease status, and therapeutic aspects to elucidate the reason that older female patients are resistant to a combination of PEG-IFN and RBV therapy in CHC with a high viral load genotype 1b.

In conclusion, our results demonstrated that wild type core aa 70, two or more aa mutations in the ISDR, low viral load, high PLT counts, and male gender are useful markers for predicting SVR.

Acknowledgments We express our thanks to other members of the Study Group of Optimal Treatment of Viral Hepatitis: Hideyuki Nomura, Shin-Kokura Hospital; Yoshiyuki Ueno, University of Tohoku; Hisataka Moriwaki, Gifu University; Makoto Oketani, Kagoshima University Graduate School of Medical and Dental Sciences; Masataka Seike, Oita University; Hiroshi Yotsuyanagi, The University of Tokyo. This study was supported in part by a Grant-in-Aid from the Ministry of Health, Labor and Welfare, Japan.

References

1. Manns MP, McHutchinson JG, Gordon SC, Rustgi VK, Shiffman M, Reindollar R, et al. Peginterferon alfa-2b plus ribavirin for initial treatment of chronic hepatitis C: a randomized trial. Lancet. 2001;358:958–65.
2. Fried MW, Shiffman ML, Reddy KR, Smith C, Marinos G, Gonzales FL, et al. Peginterferon alfa-2a plus ribavirin for chronic hepatitis C virus infection. N Engl J Med. 2002;347:975–82.
3. Hadziyannis S, Sette H Jr, Morgan TR, Balan V, Diago M, Marcellin P, et al. Peginterferon-alfa-2a plus ribavirin combination therapy in chronic hepatitis C. a randomized study of treatment duration and ribavirin dose. Ann Intern Med. 2004;40:346–55.
4. Hiramatsu N, Kurashige N, Oze T. Takehara T, Tamura S, Kasahara A, et al. Early decline of hemoglobin can predict progression of hemolytic anemia during pegylated interferon and ribavirin combination therapy in patients with chronic hepatitis C. Hepatol Res. 2008;38:52–9.
5. Honda T, Katano Y, Urano F, Murayama M, Hayashi K, Ishigami M, et al. Efficacy of ribavirin plus interferon-α in patients aged 60 years with chronic hepatitis C. J Gastroenterol Hepatol. 2007;22:989–95.
6. Sezaki H, Suzuki F, Kawamura Y, Yatsuji H, Hosaka T, Akuta N, et al. Poor response to pegylated interferon and ribavirin in older women infected with hepatitis C virus of genotype 1b in high viral load. Dig Dis Sci 2009;54:1317–24
7. Puoti C, Castellacci R, Montagness F, Zaltron S, Stornaiuolo G, Bergami N, et al. Histological and virological features and follow-up of HCV carriers with normal aminotransferase levels: the Italian Study of the Asymptomatic C Carriers (ISACC). J Hepatol. 2002;37:117–23.
8. Hui CK, Belaye T, Montegrande K, Wright TL. A comparison in the progression of liver fibrosis in chronic hepatitis C between persistently normal and elevated transaminase. J Hepatol. 2003;38:511–7.
9. Okanoue T, Makiyama A, Nakayama M, Sumida Y, Mitsuyoshi H, Nakajima T, et al. A follow-up study to determine the value of liver biopsy and need for antiviral therapy for hepatitis C virus carriers with persistently normal serum aminotransferase. J Hepatol. 2005;43:599–605.
10. Bressler BL, Guindi M, Tomlinson G, Heathcote J. High body mass index in an independent risk factor for non response to antiviral treatment in chronic hepatitis C. Hepatology. 2003;38:639–44.
11. Walsh MJ, Jonsson JR, Richardson MM, Lipka GM, Purdi DM, Clouston AD, et al. Non-response to antiviral therapy is associated with obesity and increased hepatic expression of suppressor of cytokine signaling 3 in patients with chronic hepatitis C, viral genotype 1. Gut. 2006;55:604–9.
12. Patton HM, Patel K, Behling C, Bylund C, Blatt LM, Vallee M, et al. The impact of steatosis on disease progression and early and sustained treatment response in chronic hepatitis C patients. J Hepatol. 2004;40:484–90.
13. Asselah T, Rubbia-Brandt L, Marcellin M, Negro F. Steatosis in chronic hepatitis C: why does it really matter? Gut. 2006; 55:123–30.
14. Romero-Gomez M, Del Mar Viloria M, Andrade RJ, Salmeron J, Diago M, Fernandez-Rodriguez CM, et al. Insulin resistance impairs sustained response rate to peginterferon plus ribavirin in chronic hepatitis C patients. Gastroenterology. 2005;128: 636–41.
15. Bruno S, Camma C, Di Marco V, Rumi M, Vinci M, Cammozzi M, et al. Peginterferon alfa-2b plus ribavirin for native patients with genotype 1 chronic hepatitis C: a randomized controlled trial. J Hepatol. 2004;41:474–81.
16. Everson GT, Hoefs JC, Seeff LB, Bonkovsky HL, Naishadham D, Shiffman ML, et al. Impact of disease severity on outcome of antiviral therapy for chronic hepatitis C: lessons from the HALT-C trial. Hepatology. 2006;44:1675–84.
17. McHutchison JG, Manns M, Patel K, Poynard T, Lindsay KL, Trepo C, et al. Adherence to combination therapy enhances sustained response in genotype-1-infected patients with chronic hepatitis C. Gastroenterology. 2002;123:1061–9.
18. Jeffers LJ, Cassidy W, Howell CD, Hu S, Reddy R. Peginterferon alfa-2a (40kd) and ribavirin for black American patients with chronic HCV genotype 1. Hepatology. 2004;39:1702–6.
19. Muir AJ, Bornstein JD, Killenberg PG, Atlantic Coast Hepatitis Treatment Group. Peginterferon alfa 2b and ribavirin for the treatment of chronic hepatitis C in blacks and non-Hispanic whites. N Engl J Med. 2004;350:2265–71.
20. Poynard T, Marcellin P, Lee SS, Niederau C, Minuk GS, Ideo G, et al. Randomized trial of interferon alpha 2b plus ribavirin for 48 weeks or 24 weeks versus interferon alpha 2b plus placebo for 48 weeks for treatment for chronic infection with hepatitis C virus. International Hepatitis Interventional Therapy Group (IHIT). Lancet. 1998;352:1426–32.
21. Enomoto N, Sakuma I, Asahina Y, Kurosaki M, Murakami T, Yamamoto C, et al. Mutations in the nonstructural protein 5 A gene and response to interferon in patients with chronic hepatitis C virus 1b infection. N Engl J Med. 1996;334:77–81.
22. Akuta N, Suzuki F, Sezaki H, Suzuki Y, Hosaka T, Someya T, et al. Association of amino acid substitution pattern in core protein of hepatitis C virus genotype 1b high viral load and non-virological response in interferon-ribavirin combination therapy. Intervirology. 2005;48:372–80.
23. Donlin MJ, Cannon NA, Yao E, Li J, Wahed A, Taylor MW, et al. Pretreatment sequence diversity differences in the

full-length hepatitis C virus open reading frame correlate with early response to therapy. J Virol. 2007;81:8211–24.
24. Davis GL, Wong JB, McHutchison JG, Manns MP, Harvey J, Albrecht J. Early virologic response to treatment with peginterferon alfa-2b plus ribavirin in patients with chronic hepatitis C. Hepatology. 2003;38:645–52.
25. Ferenci P, Fried MW, Shiffman ML, Smith CI, Marinos G, Goncales FL, et al. Predicting sustained virological responses in chronic hepatitis C patients treated with peginterferon alfa-2a ribavirin. J Hepatol. 2005;43:425–33.
26. Moucari R, Ripault M-P, Oules V, Martinot-Peignoux M, Asselah T, Boyer N, et al. High predictive value of early viral kinetics in retreatment with peginterferon and ribavirin of chronic hepatitis C patients non-responders to standard combination therapy. J Hepatol. 2007;46:596–604.
27. Akuta N, Suzuki F, Kawamura Y, Yatsuji H, Sezaki H, Suzuki Y, et al. Predictive factors of early and sustained responses to peginterferon plus ribavirin combination therapy in Japanese patients infected with hepatitis C virus genotype 1a: amino acid substitutions in the core region and low-density lipoprotein cholesterol level. J Hepatol. 2007;46:403–10.
28. Desmet VJ, Gerber M, Hoofnagle JH, Manna M, Scheuer PJ. Classification of chronic hepatitis: grading and staging. Hepatology. 1994;19:1513–20.
29. Kato N, Hijikata M, Ootsuyama Y, Nakagawa M, Ohkoshi S, Sugimura T, et al. Molecular cloning of the human hepatitis C virus genome from Japanese patients with non-A, non-B hepatitis. Proc Natl Acad Sci USA. 1990;87:9524–8.
30. Okanoue T, Itoh Y, Minami M, Sakamoto S, Yasui K, Sakamoto M, et al. Interferon therapy lowers the rate of progression to hepatocellualr carcinoma in chronic hepatitis C but not significantly in an advanced stage: a retrospective study in 1148 patients. J Hepatol. 1999;30:653–9.
31. Okanoue T, Itoh Y, Minami M, Hashimoto H, Yasui K, Yotsuyanagi H, et al. Guidelines for the antiviral therapy of hepatitis C virus carriers with normal serum aminotransferase based on platelet count. Hepatol Res. 2008;38:27–36.
32. Iwasaki Y, Ikeda H, Araki Y, Osawa T, Kita K, Ando M, et al. Limitation of combination therapy of interferon and ribavirin for older patients with chronic hepatitis. Hepatology. 2006;43:54–63.
33. El-Shamy A, Nagano-Fujii M, Sasase N, Imoto S, Kim SR, Hotta H. Sequence variation in hepatitis C virus nonstructural protein 5A predicts clinical outcome of pegylated interferon/ribavirin combination therapy. Hepatology. 2008;48:38–47.
34. Patton HM, Patel K, Behling C, Bylund D, Blatt LM, Vallee M, et al. The impact of steatosis on disease progression and early and sustained treatment response in chronic hepatitis C patients. J Hepatol. 2004;40:484–90.
35. Lagging M, Romero A, Westin J, Norkrans G, Dhillon AP, Palwlosky JM, et al. IP-10 predicts viral response and therapeutic outcome in difficult-to-treat patients with HCV genotype 1 infection. Hepatology. 2006;44:1617–25.
36. Pilli M, Zerbini A, Penna A, Orlandini A, Lukasiewicz E, Pawlotsky JM, et al. HCV-specific T-cell response in relation to viral kinetics and treatment outcome (DITTO-HCV Project). Gastroenterology. 2007;133:1132–43.
37 Shirakawa H, Matsumoto A, Joshita S, Komatsu M, Tanaka N, Umemura T, et al. Pretreatment prediction of virological response to peginterferon plus ribabirin therapy in chronic hepatitis C patients using viral and host factors. Hepatology. 2008; 48:1753–60.

Oncogene (2009) 28, 2910–2918

www.nature.com/onc

ORIGINAL ARTICLE

Defective expression of polarity protein PAR-3 gene (*PARD3*) in esophageal squamous cell carcinoma

K Zen[1], K Yasui[1], Y Gen[1], O Dohi[1], N Wakabayashi[1], S Mitsufuji[1], Y Itoh[1], Y Zen[2], Y Nakanuma[2], M Taniwaki[3], T Okanoue[1,4] and T Yoshikawa[1]

[1]*Department of Molecular Gastroenterology and Hepatology, Graduate School of Medical Science, Kyoto Prefectural University of Medicine, Kyoto, Japan;* [2]*Department of Human Pathology, Kanazawa University Graduate School of Medicine, Kanazawa, Japan;* [3]*Department of Molecular Hematology and Oncology, Graduate School of Medical Science, Kyoto Prefectural University of Medicine, Kyoto, Japan and* [4]*Department of Hepatology, Saiseikai Suita Hospital, Suita, Japan*

The partition-defective 3 (PAR-3) protein is implicated in the formation of tight junctions at epithelial cell–cell contacts. We investigated DNA copy number aberrations in human esophageal squamous cell carcinoma (ESCC) cell lines using a high-density oligonucleotide microarray and found a homozygous deletion of *PARD3* (the gene encoding PAR-3). Exogenous expression of *PARD3* in ESCC cells lacking this gene enhanced the recruitment of zonula occludens 1 (ZO-1), a marker of tight junctions, to sites of cell–cell contact. Conversely, knockdown of *PARD3* in ESCC cells expressing this gene caused a disruption of ZO-1 localization at cell–cell borders. A copy number loss of *PARD3* was observed in 15% of primary ESCC cells. Expression of *PARD3* was significantly reduced in primary ESCC tumors compared with their nontumorous counterparts, and this reduced expression was associated with positive lymph node metastasis and poor differentiation. Our results suggest that deletion and reduced expression of *PARD3* may be a novel mechanism that drives the progression of ESCC.
Oncogene (2009) **28,** 2910–2918; doi:10.1038/onc.2009.148; published online 8 June 2009

Keywords: PAR-3; *PARD3*; esophageal squamous cell carcinoma; homozygous deletion; tight junction; metastasis

Introduction

Esophageal cancer is the sixth leading cause of cancer mortality worldwide (Enzinger and Mayer, 2003). Of the two main histological subtypes of esophageal cancer, squamous cell carcinoma is prevalent worldwide, although the incidence of adenocarcinoma has been increasing in North America and Europe (Vizcaino *et al.*, 2002).

Correspondence: Dr K Yasui, Department of Molecular Gastroenterology and Hepatology, Graduate School of Medical Science, Kyoto Prefectural University of Medicine, 465 Kajii-cho, Kamigyo-ku, Kyoto 602-8566, Japan.
E-mail: yasuik@koto.kpu-m.ac.jp
Received 9 December 2008; revised 13 April 2009; accepted 7 May 2009; published online 8 June 2009

Inactivation of tumor suppressor genes is critical to the development and progression of human malignancies. Much effort has been put into finding homozygous deletions in cancer cells in the expectation that they harbor tumor suppressor genes. Suppressor genes that have been identified partly from homozygous deletions include *CDKN2A* (Kamb *et al.*, 1994), *PTEN* (Li *et al.*, 1997) and *SMAD4* (Hahn *et al.*, 1996). The recent introduction of high-density oligonucleotide microarrays designed for typing of single nucleotide polymorphisms (SNPs) facilitates high-resolution mapping of chromosomal amplifications, deletions and losses of heterozygosity (Mei *et al.*, 2000; Zhao *et al.*, 2004).

Cell polarization and the formation of cell–cell junctions are coupled processes that are essential to tissue morphogenesis (Macara, 2004). Loss of cell–cell adhesion and cell polarity is commonly observed in advanced tumors and correlates strongly with their invasion into adjacent tissues and the formation of metastases (Wodarz and Näthke, 2007).

It has become apparent that polarity is largely regulated by a conserved set of proteins referred to as partition-defective (PAR) proteins (Kemphues *et al.*, 1988; Macara, 2004; Suzuki and Ohno, 2006). These proteins were first identified in the zygote of *Caenorhabditis elegans*, where they specify the anterior–posterior body axis. They are also essential for asymmetric cell division in *Drosophila melanogaster*. The mammalian homologs of the *C. elegans* polarity proteins have evolutionarily conserved functions in the establishment of cell polarity in various cell types. One of these homologs, PAR-3, contains one self-oligomerization domain in the N terminus, three PDZ protein interaction domains and one atypical protein kinase C (aPKC)-binding domain (Izumi *et al.*, 1998; Joberty *et al.*, 2000; Lin *et al.*, 2000; Assémat *et al.*, 2008). These domains enable PAR-3 to form a conserved protein complex with PAR-6 and aPKC (Macara, 2004; Suzuki and Ohno, 2006). In mammalian epithelial cells, this PAR-3–PAR-6–aPKC complex assembles at tight junctions, where it is necessary for the establishment of apico-basal polarity.

Thus, deletion of PAR protein genes in tumor cells may disrupt cell polarity and adhesion. To identify the

genes that are potentially involved in human esophageal squamous cell carcinoma (ESCC), we investigated DNA copy number aberrations in ESCC cell lines using high-resolution SNP arrays. We show that the gene encoding human PAR-3 protein, *PARD3*, is homozygously deleted in ESCC cells, and that this deletion affects the formation of tight junctions in these cells. Furthermore, we show that reduced expression of *PARD3* is associated with the aggressiveness of primary ESCC tumors.

Results

Identification of homozygous deletion of PARD3

To identify genes potentially involved in ESCC, we screened for DNA copy number aberrations in 20 ESCC cell lines by Affymetrix GeneChip Mapping 250K array analysis. Of the 20 cell lines screened, KYSE30 and KYSE270 cells exhibited homozygous deletions at the chromosomal region 10p11 (Figure 1a). The estimated extent of the common region of deletion was ~280 kb between the markers SNP_A-2051960 and SNP_A-1867256, which includes a single gene *PARD3* (Supplementary Figure S1). The extent of the shortest region of overlap of homozygous deletions was narrowed down to exons 3–22 of *PARD3* by genomic PCR analyses (Figures 1b and c).

Copy number and expression of PARD3 *in ESCC cell lines*

We analysed the DNA copy number and expression level of *PARD3* in 20 ESCC cell lines and normal lymphocytes and in esophageal epithelial cells as a control (Figure 2). Comparison with normal esophageal epithelial cells showed lower expression of *PARD3* in 18 of the 20 ESCC cell lines (Figure 2b). The absence of the *PARD3* gene in the KYSE30 and KYSE270 cell lines was confirmed by real-time quantitative reverse transcription (RT)–PCR and immunoblot analyses. These assays did not detect the expression of *PARD3* mRNA and the PAR-3 protein, respectively (Figures 2b and c). Analyses of the cell lines by real-time quantitative RT–PCR and immunoblot indicated varying expression levels of *PARD3* mRNA, and three forms of the PAR-3 protein with molecular weights of 180, 150 and 100 kDa, respectively (Figures 2b and c).

PAR-3-dependent recruitment of ZO-1 to sites of cell–cell contact in ESCC cells

To determine whether the deletion of *PARD3* leads to defective tight junction formation in ESCC cells, we determined the effect of *PARD3* deletion on the subcellular localization of zonula occludens 1 (ZO-1), a marker of cellular tight junctions (Stevenson *et al.*, 1986). For this purpose, we compared the colocalization

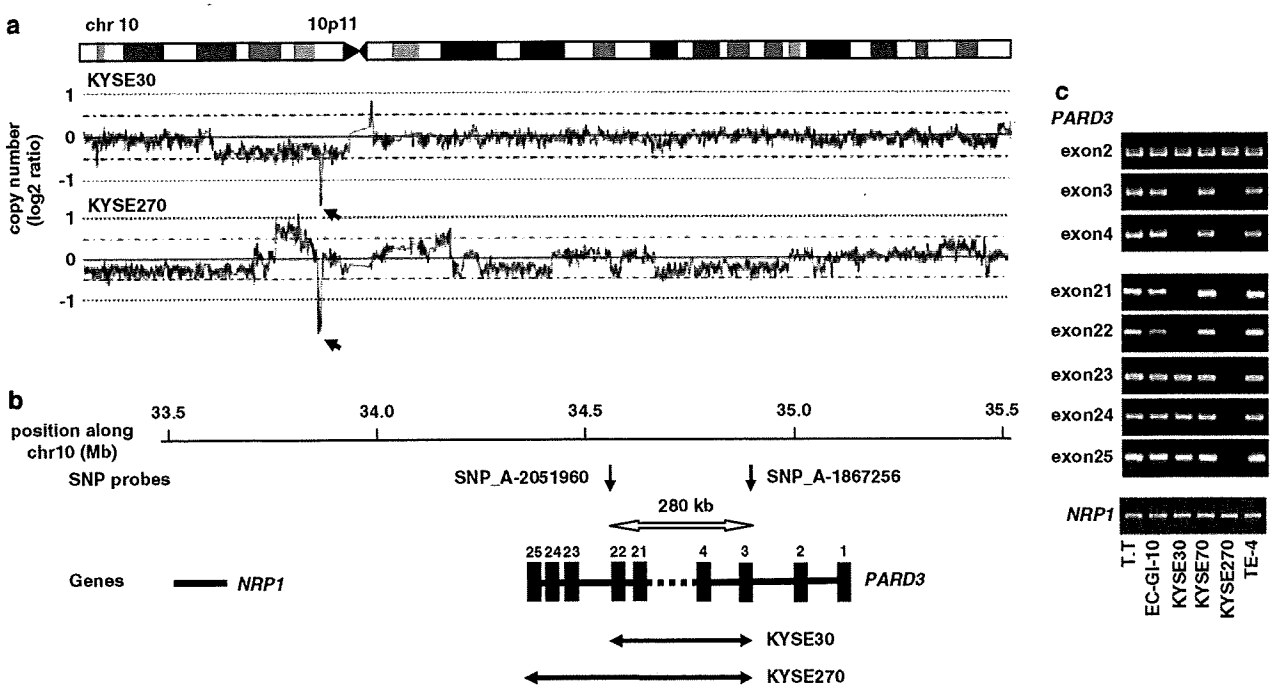

Figure 1 Homozygous deletion of *PARD3* in ESCC cell lines. (a) Chromosome 10 cytoband map and copy numbers determined by Affymetrix GeneChip Mapping 250K arrays of KYSE30 and KYSE270 cells. Arrows indicate the loci for homozygous deletions at position 10p11. (b) Map of 10p11 encompassing the region that is homozygously deleted in KYSE30 and KYSE270 cells. The position of the Affymetrix SNP probes, the two genes (*NRP1* and *PARD3*) and the exons of *PARD3* is shown according to the UCSC genome database 2006 (http://genome.ucsc.edu/). Horizontal arrows indicate the regions homozygously deleted in KYSE30 and KYSE270 cells as determined by genomic PCR analyses (see panel c). The horizontal white closed arrow indicates the minimal common region of deletion. (c) PCR analysis of each exon of the *PARD3* and *NRP1* genes using a genomic DNA template derived from six ESCC cell lines.

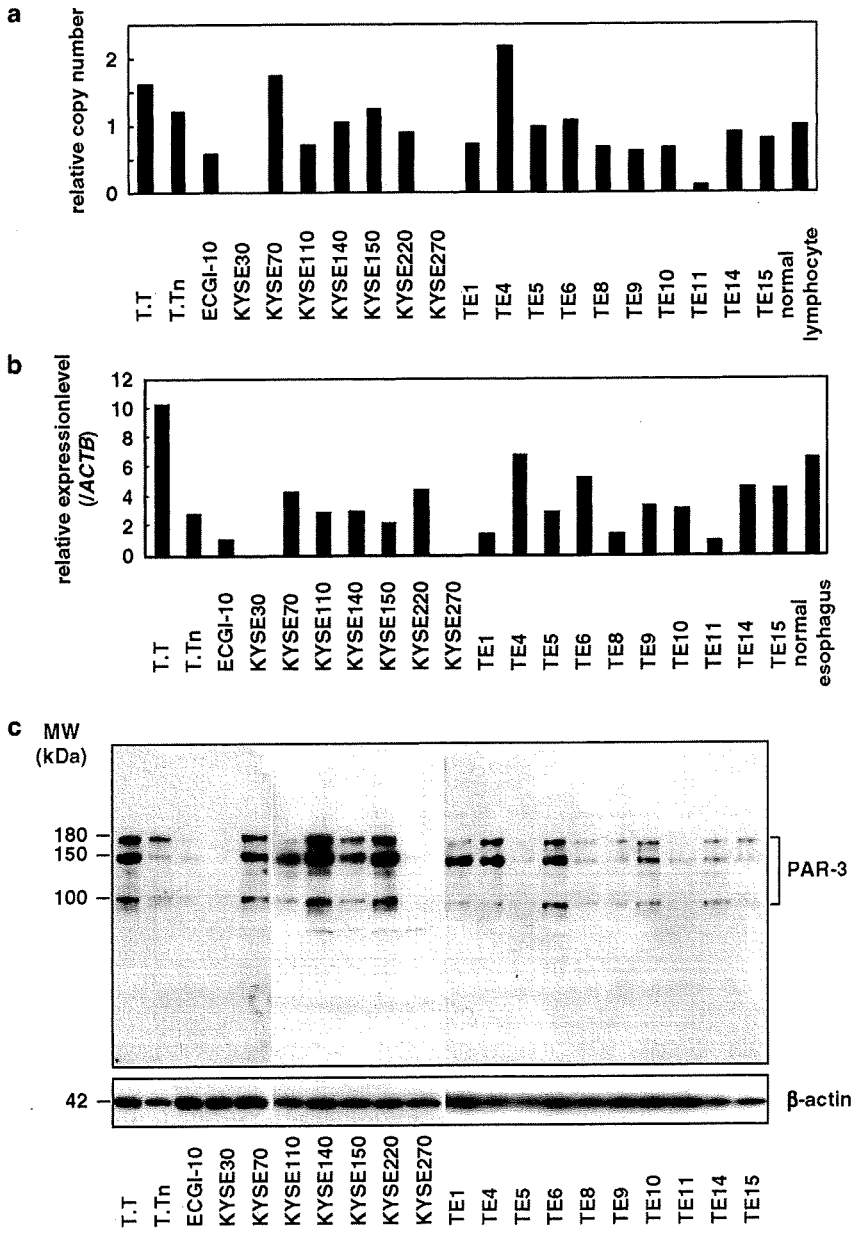

Figure 2 Copy number and expression level of *PARD3* in 20 ESCC cell lines. (a) The copy number of *PARD3* in 20 ESCC cell lines as measured by real-time quantitative PCR with reference to the LINE-1 control. Values are normalized such that the copy number in genomic DNA derived from normal lymphocytes has a value of 1. (b) Relative expression levels of *PARD3* in 20 ESCC cell lines and normal esophagus as evaluated by real-time quantitative reverse transcription (RT) PCR. The results are presented as the expression level of each gene relative to a reference gene (*ACTB*) in order to correct for variations in the amount of RNA. (c) Immunoblot analyses of protein levels of PAR-3 in the indicated cell lines. β-Actin was used as an internal control.

of PAR-3 and ZO-1 by immunofluorescence in two *PARD3*-expressing cell lines (T.T and TE-4) with that in two cell lines lacking *PARD3* (KYSE30 and KYSE270). ZO-1 colocalized with PAR-3 at sites of cell–cell contact in T.T and TE-4 cells (Figure 3a). In contrast, ZO-1 was only weakly observed at sites of cell–cell contact in KYSE30 cells and was barely detected in KYSE270 cells (Figure 3a), despite the fact that the ZO-1 protein could be detected by immunoblotting in all cell lines (Figure 3b). As expected, the expression of PAR-3 was not detected in KYSE30 or KYSE270 cells (Figure 3a).

To further confirm that the absence of PAR-3 was the cause of the aberrant localization of ZO-1 in the KYSE30 and KYSE270 cells, we determined whether transfection of *PARD3* into these cells could restore ZO-1 localization to tight junctions. After transfection, the expression of PAR-3 (molecular weight, 180 kDa) in the *PARD3*-transfected KYSE30 and KYSE270 cells was detected by immunoblotting analysis (Figure 4a).